Inelastic neutron scattering, phonon softening, and the phase transition in sodium nitrate, $NaNO_3$

1998 J. Phys.: Condens. Matter 10 6851

(http://iopscience.iop.org/0953-8984/10/30/022)

J. Phys.: Condens. Matter **10** (1998) 6851–6861. Printed in the UK PII: S0953-8984(98)89646-X

Inelastic neutron scattering, phonon softening, and the phase transition in sodium nitrate, $NaNO_3$

M J Harris†, M E Hagen‡, M T Dove§ and I P Swainson‖

† ISIS Facility, Rutherford Appleton Laboratory, Chilton, Didcot, Oxfordshire OX11 0QX, UK
‡ Department of Physics, Keele University, Keele, Staffordshire ST5 5BG, UK
§ Mineral Physics Group, Department of Earth Sciences, University of Cambridge, Cambridge CB2 3EQ, UK
‖ Neutron Program for Materials Research, Steacie Institute for Molecular Sciences, National Research Council, Chalk River Laboratories, Chalk River, Ontario K0J 1P0, Canada

Received 1 December 1997, in final form 3 April 1998

Abstract. Neutron scattering measurements have been performed on sodium nitrate ($NaNO_3$) at temperatures between 16 and 553 K, using both time-of-flight and triple-axis spectrometers, focusing on the phonon modes with wavevectors between the Brillouin zone centre and the F zone boundary point. At the F point there is a significant softening in energy of a transverse acoustic phonon branch on heating. Unlike the case of the related material calcite, there is no continuum of inelastic scattering localized in reciprocal space about the F point, and with a strong temperature dependence. Instead we find a component of inelastic scattering that is broad in both energy and wavevector, and with only a weak dependence on temperature.

1. Introduction

Sodium nitrate ($NaNO_3$) undergoes an orientational order–disorder phase transition at 549 K with the symmetry change $R\bar{3}c \rightarrow R\bar{3}m$ on heating. This symmetry change is marked by the disappearance of superlattice reflections at the Z points of reciprocal space (i.e. the (0 0 1.5) point indexed using the hexagonal setting of $R\bar{3}m$). In the high-temperature phase the nitrate molecular ions are disordered with respect to 60° reorientations about their threefold axes. The phase transition has been studied experimentally by x-ray diffraction [1–3], neutron diffraction [4], Raman and infrared spectroscopy [5–9], inelastic neutron scattering [10, 11], birefringence measurements [12], and measurements of lattice parameters [13], and theoretically by molecular dynamics simulations [14]. A very similar phase transition occurs in the mineral calcite, $CaCO_3$, at 1260 K [15, 16], so both $NaNO_3$ and calcite have the same ordered and disordered structures above and below their respective phase transition temperatures. In both cases, ordering induces a large spontaneous strain ϵ_3 [13, 15]. Moreover, the macroscopic representation of the order parameter, Q, extracted from macroscopic experimental measurements such as measurements of x-ray superlattice intensities [2, 15], birefringence [12], and spontaneous strain [13, 15], follows a classical tricritical temperature dependence over a wide range of temperatures for both compounds:

$$Q = Q_0|T_c - T|^{\beta} \tag{1}$$

with $\beta = 0.25$ [2, 12, 13, 15]. However, for $NaNO_3$ (but not in calcite), the value of β is lowered to 0.22 over a temperature range of $\simeq$30 K close to T_c. A recent neutron diffraction

0953-8984/98/306851+11$19.50

study of the critical scattering from $NaNO_3$ has shown that an additional crossover occurs about 5 K below T_c, where the order parameter changes to $\beta = 0.41$ [17]. Above T_c, two Lorentzian components to the critical scattering at the Z point were observed. One was broad in wavevector, and appeared to be non-critical. What is unclear is why the β-exponent changes, or indeed, why it is close to being tricritical to begin with.

It may be that the change in the value of β from 0.25 to 0.22 is due to critical fluctuations, but it is generally the case that for tricritical phase transitions the marginal dimension is 3 [18], so the effect of critical fluctuations should be only to add small logarithmic corrections to the temperature dependence of Q rather than to change the value of β over such a wide temperature interval. Schmahl and Salje [2] have instead suggested that the change in the value of β is due to the existence of fluctuations of the structure into a different ordered phase, and their numerical analysis of x-ray diffraction data within the formalism of Landau theory is compatible with such a model. However, the question of why the transitions in both $NaNO_3$ and $CaCO_3$ are close to tricritical remains to be answered. In many cases, tricritical phase transitions arise through an accidental vanishing of the fourth-order term in the free energy due to coupling of Q with the strain [18], but such an accidental vanishing is unlikely to occur for *both* $NaNO_3$ and $CaCO_3$.

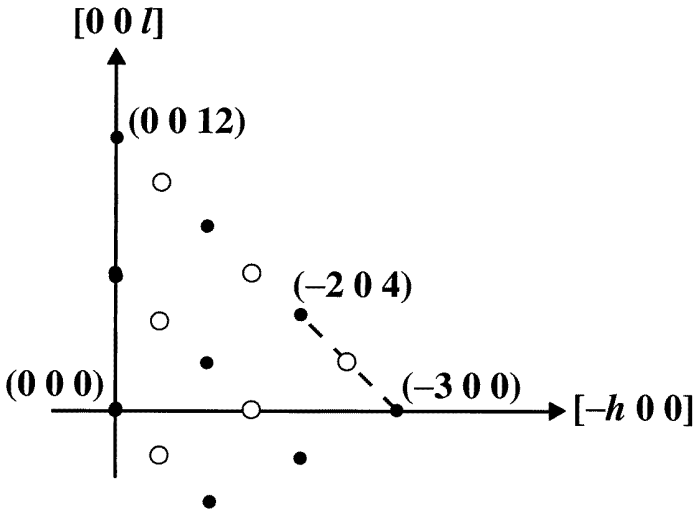

Figure 1. The a^*–c^* plane of reciprocal space for $NaNO_3$, with some of the Bragg points of the low-temperature phase labelled. The filled circles represent Bragg reflections, and the open circles represent F points of the high-temperature Brillouin zone. The axes are shown for the low-temperature form. The dashed line shows the trajectories of the inelastic scans shown in figure 2 (see later), projected onto the a^*–c^* plane.

In our search for an explanation of the tricritical nature of both phase transitions, we have focused on another feature observed for both $NaNO_3$ and $CaCO_3$, namely the existence of strong x-ray diffuse scattering associated with the positions corresponding to the F points on the surfaces of the Brillouin zones of the high-temperature phases [1, 3] (i.e. the point (0.5 0 2) in the hexagonal setting, noting that the Bragg peaks exist for $-h + k + \ell = 3n$; figure 1). This diffuse scattering has been observed for the *low-temperature* phases of both materials. In both $NaNO_3$ and $CaCO_3$ there is a softening of a transverse acoustic mode at this wavevector on heating toward the transition temperature [11, 19]. A possible interpretation of the diffuse scattering is that it arises from the existence of small domains of

the material with different orientational ordering and translational symmetry, such that the F point would become a reciprocal-lattice vector. This interpretation provided the motivation for the work of Schmahl and Salje [2]. Given that multi-component order parameters can give rise to fluctuation-induced first-order phase transitions when second-order transitions are allowed by symmetry, it may be that the existence of competing order parameters can give rise to the tricritical phase transitions observed in both $NaNO_3$ and $CaCO_3$. We have investigated the experimental situation in calcite further by performing extensive inelastic neutron scattering measurements [19, 20]. The principal new feature observed in these measurements was the existence of a continuum of inelastic scattering strongly localized at the F point, with a strong temperature dependence.

Calcite is a difficult material to study experimentally due to the chemical dissociation of the carbonate ion at temperatures below the transition temperature. For this reason, $NaNO_3$ has been studied as an analogue of calcite, and the present work was initially undertaken in order to examine whether a similar anomalous inelastic spectrum exists for $NaNO_3$ and to investigate its temperature dependence close to and above the transition temperature. We have found that the inelastic spectra of $NaNO_3$ are not just different from those of calcite in the fine detail, but they are also *qualitatively* different, as will be described in section 3.

2. Experimental details

Our inelastic neutron scattering measurements were performed on two separate instruments: the multi-analyser time-of-flight spectrometer PRISMA at the ISIS spallation neutron source, and the N5 triple-axis spectrometer at the NRU reactor at Chalk River, Canada (operated by AECL research). PRISMA has been described in detail by Steigenberger *et al* [21], and our experimental set-up was very similar to that used in our previous study of calcite [19, 20]. The spectra are collected on PRISMA along a path in which both the wavevector transfer $\boldsymbol{Q}$ and energy transfer E vary. With the use of several analysers and detectors, the time-of-flight nature of these measurements allows a series of $\boldsymbol{Q}$–E trajectories to be measured simultaneously, thereby allowing extensive sets of phonon dispersion curves to be obtained with a single setting of the spectrometer.

In the PRISMA experiments, we used two different crystals, one with an approximate volume of 2 cm^3, and the other with an approximate volume of 20 cm^3. Both crystals were mounted with the $\boldsymbol{a}^*$–$\boldsymbol{c}^*$ plane in the scattering plane of the spectrometer. In both cases we used 14 analyser–detector arms on the spectrometer. The first experiment utilized the (1 1 1) Bragg peak reflections from a germanium crystal for energy analysis, and the second used the (0 0 2) Bragg reflection from a pyrolytic graphite crystal. The analysing energies used on the 14 analyser–detector arms were in the range 20 to 53 meV.

During the first experiment the crystal was cooled to 16 K using a closed-cycle refrigerator, and the temperature was monitored using a Rh–Fe resistance thermometer. We also heated this crystal up to the transition temperature, but we discovered that, since the melting point is only about 25 K above T_c, the inelastic spectrum is sensitive to the thermal treatment, so the intensity (although not the profile) decays on cycling the temperature. For this reason we repeated our measurements using a new crystal, and were careful only to heat in stages rather than to cycle the temperature. This crystal was heated in a vacuum furnace fitted with a K-type nickel–chromel thermocouple. The temperature control was stable to ± 1 K. All of the high-temperature measurements reported here were obtained on the second crystal. All of the features that we have observed for the second crystal were also observed for the first crystal, so we have an experimentally independent verification of our results.

We performed all of our measurements for wavevector transfers in a line along the [1 0 4] direction between the ($\bar{3}$ 0 0) and ($\bar{2}$ 0 4) reciprocal-lattice points, which takes in the F zone boundary point at ($\bar{2.5}$ 0 2). A schematic plot of the a^*–c^* plane of reciprocal space, illustrating the trajectory of these scans, is shown in figure 1. The useful range of energy transfers was from −15 to 40 meV; the spectra for larger energy transfers were contaminated by scattering from the higher-order planes of the graphite analyser crystals. The measurements at each temperature were obtained using two settings of the spectrometer. Data were collected at temperatures of 16, 300, 393, 473, 513, 533, 543 and 553 K. The intensities of the spectra from the different detectors were normalized using the incoherent elastic scattering from a vanadium sample.

A careful assessment of the background scattering was carried out in two different ways. In the first method the sample was kept in place, and the analyser crystals were rotated by 2° from their Bragg reflection condition. This type of measurement was performed to assess how much, if any, scattering from the sample was incoherently scattered by the analyser crystals. We note that the incoherent cross sections for neutron scattering from germanium and pyrolytic graphite are small, but we felt that it was important to check this possibility, since if it did occur it would lead to an *apparent* broad inelastic spectrum. The measurements carried out showed that there was no significant amount of scattering through this process. The second type of background measurement was carried out with the crystal removed but with the sample holder in place. The background spectra were flat over the range −15 to 40 meV except close to the elastic line due to scattering from the tantalum band used to secure the crystal in place. This scattering did not significantly interfere with our measurements. In both cases the background spectra were obtained using the same spectrometer settings as were used for data collection.

A smaller number of measurements were performed on the same crystals using the N5 triple-axis spectrometer on the NRU reactor at Chalk River, Canada (operated by AECL research). All of these measurements were taken at room temperature, and were principally designed to confirm the results obtained with PRISMA. The N5 spectrometer was operated in constant-$\boldsymbol{Q}$ mode with fixed analysing energy (E_f). The monochromator crystal was silicon, scattering from a (1 1 1) face, and the analysing crystal was pyrolytic graphite (0 0 2). We used two values of E_f, 14.5 and 29 meV—the first was used for the measurement of phonon energies, since it has a reasonably high resolution, and the second was used to investigate broader features discovered in the PRISMA experiments. The analysing energy of $E_f = 29$ meV (and hence also the energy resolution) was similar to that used in our PRISMA experiments.

3. Results and discussion

3.1. PRISMA results and the broad picture

In figure 2 we show contour plots of the intensity of the inelastic neutron scattering as a function of scattering vector $\boldsymbol{Q}$ and energy transfer E for two temperatures: 300 and 553 K, with the same intensity scale used in all of the plots. The great value of these plots is that they reveal the relevant parts of the phonon dispersion curves alongside the additional features of the inelastic scattering. In this subsection we will draw out the principal points from this broad picture before homing in on the finer detail in the following subsections.

Note, first of all, that the zone centres in these contour plots are the points where $-\xi = 2$ and 3, which correspond to the ($\bar{2}$ 0 4) and ($\bar{3}$ 0 0) Bragg points, respectively. Besides the line of elastic scattering due to incoherent processes, the clearest feature in the

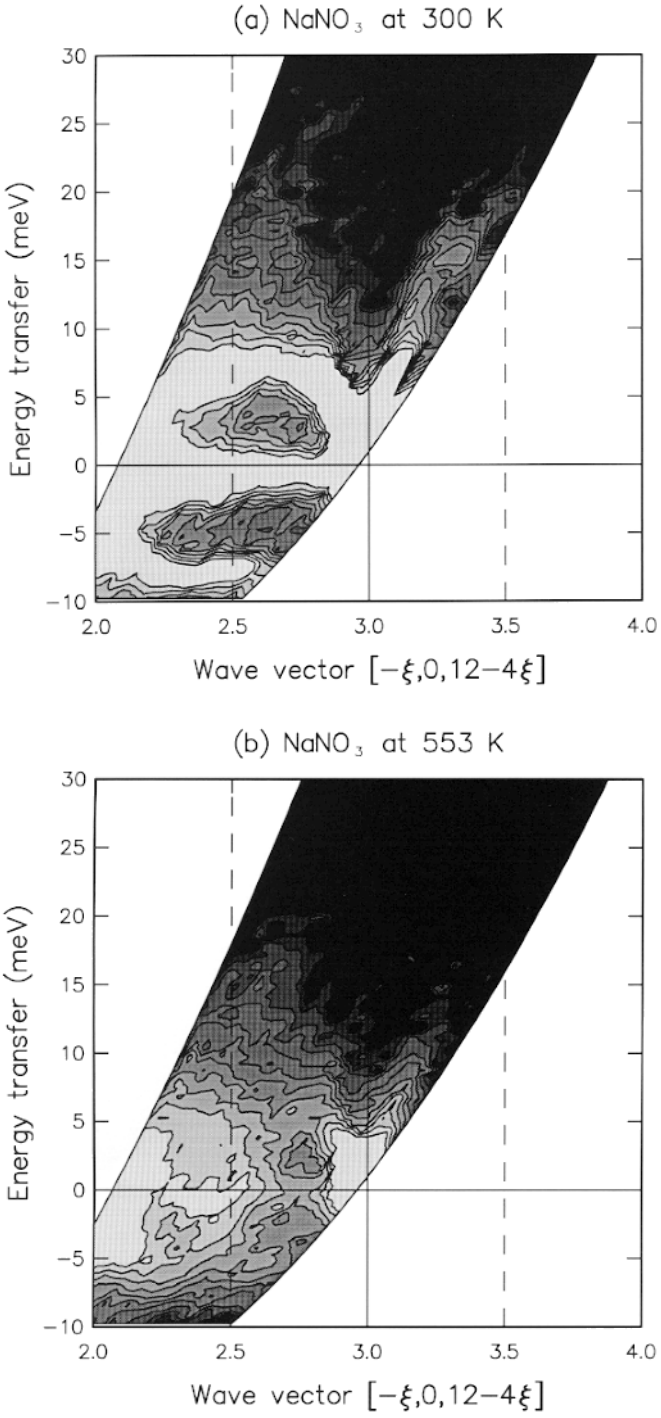

Figure 2. Contour maps of the inelastic neutron scattering from $NaNO_3$ measured at 300 and 553 K are shown in (a) and (b), respectively. The highest intensity is represented by the lightest shading, the lowest by the darkest. The background has been subtracted from these plots for clarity.

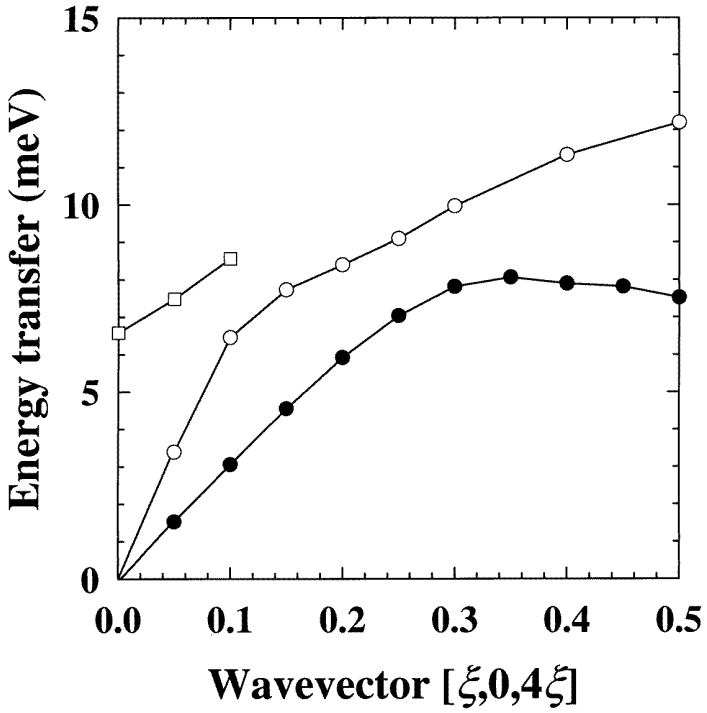

Figure 3. The low-energy phonon dispersion curves for $NaNO_3$ measured using the N5 triple-axis spectrometer at Chalk River with the sample at room temperature. Measurements were performed for wavevectors along the direction $[\xi, 0, 4\xi]$ from Γ ($\xi = 0$) to F ($\xi = 0.5$). The transverse acoustic mode is represented by the full circles, the longitudinal acoustic mode by the open circles, and the optic mode by open squares. The size of the data points represents the size of the experimental error.

contour plots is the transverse acoustic branch, which extends to about 7 meV at the zone boundary F point (where $-\xi = 2.5$) at a temperature of 300 K, but softens around the F point at higher temperatures. Less clear are the longitudinal acoustic modes, which are much weaker and can only really be identified for wavevectors close to the zone centre. Similarly, the much weaker optic modes cannot be seen in this type of measurement against the broad scattering. The triple-axis spectrometer measurements were carried out with a smaller resolution volume, which improves the discrimination of weaker sharp features against broad scattering, showing the longitudinal and optic modes clearly. The line along $E = 0$ is the elastic incoherent scattering from the Na atoms, and is of no interest here.

Aside from the observation of the phonon dispersion curves, the broad picture from the PRISMA data shows a number of other features. The effect of increasing temperature is to soften the energy of the phonon at F, but this feature is not easy to capture in the contour maps, and we will return to this below. The most significant feature is that the inelastic scattering for wavevectors around the F point is quite different from that observed in calcite. There is no trace of a continuum of inelastic scattering localized at the F point. Instead there appears to be a wide swathe of inelastic scattering that is *not* localized in reciprocal space, and which is quite unlike the scattering seen in calcite. The contour maps also suggest that the swathe of inelastic scattering is not strongly temperature dependent for temperatures between 300 and 553 K, although if the sample is cooled to 16 K it disappears.

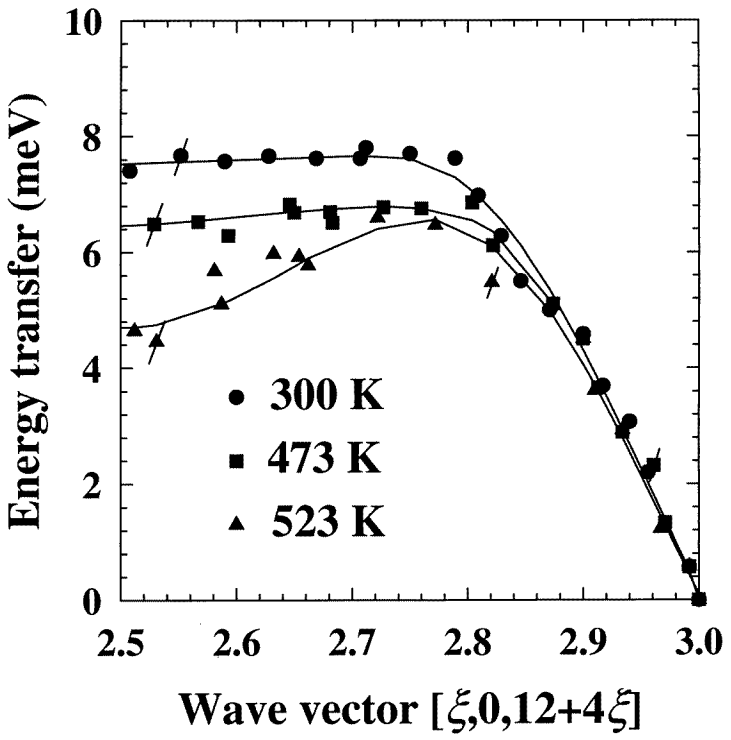

Figure 4. The phonon dispersion curves for the transverse acoustic mode with wavevectors along the line Γ–F at a number of different temperatures. The data were extracted from the PRISMA measurements. Representative error bars are shown on a number of data points.

3.2. Triple-axis spectrometer measurement of phonon dispersion curves

The triple-axis spectrometer was used to measure the low-energy phonon dispersion curves for wavevectors along the direction Γ–F using the constant-Q method. The results are shown in figure 3. The important point is the identification of the longitudinal acoustic mode, and the observation of the optic mode at around zero wavevector. These results are consistent with the PRISMA data. The low-energy phonon dispersion curves along this direction are similar to those of calcite, with the transverse acoustic branch softening around the F point, and the longitudinal acoustic branch anti-crossing with an optic branch at a wavevector close to the zone centre.

3.3. Phonons at the F zone boundary point and the effect of temperature

The contour maps of figure 2 show that the energy of the transverse acoustic phonon at the F point decreases on heating. This is highlighted in figure 4, which shows the dispersion curve for this branch at several temperatures, and in figure 5 which shows the energy of this mode at the F point as a function of temperature. The same effect was previously seen by Schmahl *et al* [11], who noted that the energy change was directly correlated with the spontaneous strain ϵ_3. We observed a similar effect in calcite [19, 20], but there are some quantitative differences, not least that this effect is somewhat stronger in calcite.

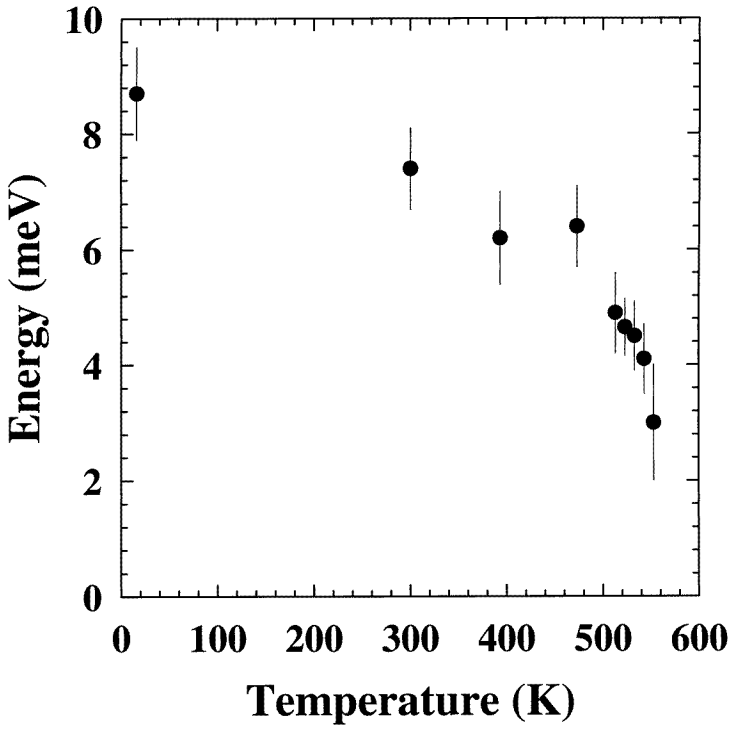

Figure 5. The energy of the transverse acoustic mode at the F point as a function of temperature. The data were extracted from the PRISMA measurements.

3.4. Additional unexplained inelastic neutron scattering

In figure 6, we show two spectra measured using the same detector on PRISMA, but with sample temperatures of 300 and 553 K. The striking feature in these spectra is the broad distribution of inelastic scattering underneath the phonon peaks. The scattering is centred on zero energy and has an energy width of $\simeq$25 meV. Similar broad scattering was found in every spectrum, in both crystals, except at a sample temperature of 16 K. Our background calibrations confirmed that this scattering arises from the sample and so must be intrinsic to the inelastic spectrum from $NaNO_3$. Although it is not particularly strong at any given energy transfer when compared to the phonon peaks, its integrated intensity is actually much higher than that of the phonons. As noted above, this scattering can be seen in the contour plots of the intensity in $\boldsymbol{Q}$–E space; see figure 2.

Although we were careful to eliminate possible spurious processes for this broad scattering, we considered it important to confirm our results by using a different instrument and technique, in this case the N5 triple-axis spectrometer. We performed constant-$\boldsymbol{Q}$ measurements at room temperature with two different fixed analysing energies, E_f = 14.5 meV and E_f = 29 meV. These two settings lead to different resolution conditions for the constant-$\boldsymbol{Q}$ scans. If simply measured in terms of the energy width of the incoherent scattering from a vanadium sample, then these two analysing energies lead to energy resolutions at $E = 0$ meV of 0.6 meV and 3 meV respectively. However, this is only part of the story: it is not just the energy resolution that changes, but also the three wavevector components of the resolution volume. It is known that the full volume of the resolution

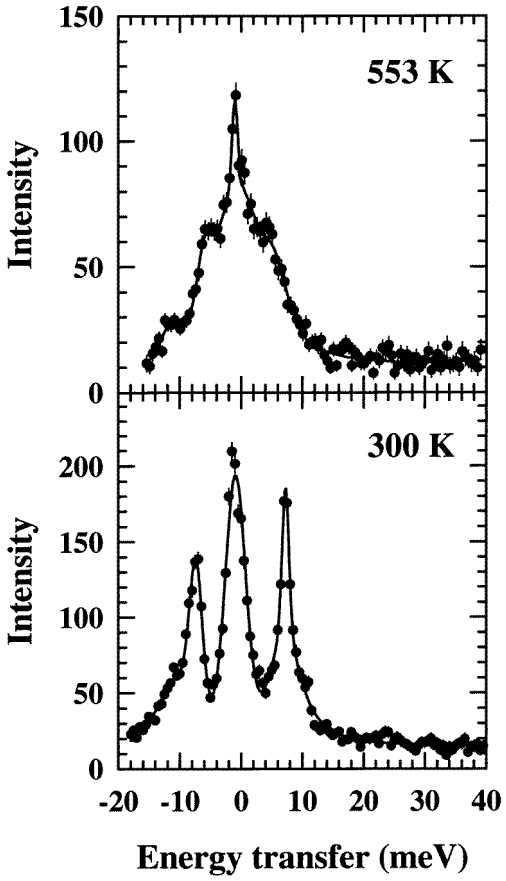

Figure 6. Single-detector spectra from the PRISMA measurements for temperatures of 300 and 553 K. A single detector cuts a parabolic trajectory through $\boldsymbol{Q}$–E space. These detector spectra go through the F point at $(\overline{2.5}\ 0\ 2)$ at zero energy transfer.

function varies approximately as the fourth power of the analysing energy [22], so the full resolution volume with $E_f = 29$ meV is roughly sixteen times that with $E_f = 14.5$ meV. This resolution volume difference means that the two sets of spectra measured with these two analysing energies will reflect the contributions from sharp features (phonon modes) and broad features quite differently. The peak intensity of a broad feature (broad compared to the resolution width) in an inelastic spectrum will scale with the resolution volume, while the peak intensity of a sharp feature (sharp, i.e. narrow, compared to the resolution width) will not. Thus, with $E_f = 14.5$ meV one might expect to observe the phonon modes very clearly, but that the peak intensity of any broad scattering would be severely attenuated by the small resolution volume. Conversely with $E_f = 29$ meV one might expect that any broad scattering will become much more intense and that sharp features would be less easy to discriminate.

A further resolution effect which must be taken into account for these two different analysing energies is the variation of the resolution volume with the energy transfer in the inelastic spectrum. The resolution volume *increases* with increasing energy transfer; however, the rate of increase of the resolution volume is different for each setting of E_f, and

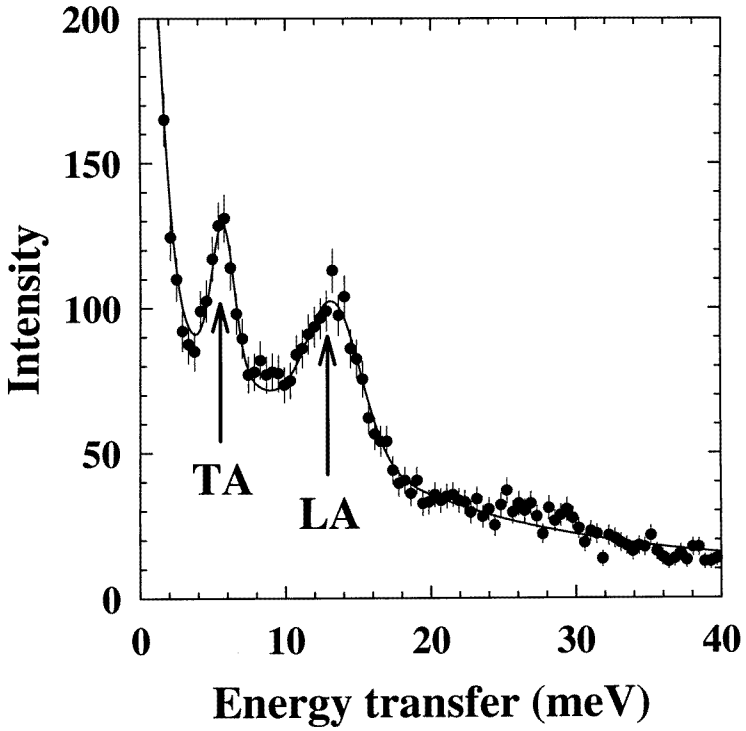

Figure 7. Constant-$\boldsymbol{Q}$ measurements of the inelastic spectra obtained on the N5 triple-axis spectrometer at the F point, measured at 300 K with $E_f = 29$ meV. The curves give a fit to the data with Gaussian functions for the phonon and elastic peaks and a Lorentzian function for the broad peak centred on zero energy transfer.

is more rapid for the lower value of $E_f = 14.5$ meV. This has the effect of distorting broad features such as the swathe. On the other hand, the resolution volume stays comparatively constant with $E_f = 29$ meV, making it a more favourable setting for observing broad features. The resolution conditions used in the PRISMA measurements are very similar to this set-up with $E_f = 29$ meV on the triple-axis spectrometer.

Results of constant-$\boldsymbol{Q}$ scans on N5 with $E_f = 29$ meV are shown in figure 7. The swathe of inelastic scattering can clearly be seen for all sets of measurements. We note that the swathe was not observed in the spectra measured with $E_f = 14.5$ meV because of the resolution effect explained above. We regard this result as confirmation of the occurrence of broad inelastic scattering underneath the phonon modes, as observed with PRISMA. It also explains why previous inelastic neutron scattering measurements did not report this swathe of scattering, since they used analysing energies of $E_f \sim 14$ meV and concentrated on measurements of the phonon modes. As a brief aside, it is also a good demonstration of how different inelastic neutron scattering techniques and spectrometers can be used to obtain complementary information, both parts of which are needed to understand the big picture.

The PRISMA contour plots in figure 2 suggest that this broad inelastic scattering does not have a significant temperature dependence above 300 K, either in intensity or width, but as noted it does disappear on cooling to 16 K. At the present time we cannot give any clear indication of the origin of this scattering. However, we note that since the

scattering is quasielastic, and has a large energy width and no strong Q-dependence, a possible explanation is that it represents fast relaxational motions of individual nitrate ions. In calcite, this process is highly correlated, resulting in the continuum of scattering localized on the F point.

4. Summary

We have presented the results of a detailed inelastic neutron scattering study of $NaNO_3$, concentrating on the excitation spectrum around the zone boundary F point. Upon heating up to and beyond the order–disorder phase transition associated with the Z point, we observe a significant softening in energy of a transverse acoustic phonon branch around the F point. A similar effect has been observed in the isostructural material calcite, but the details are different. The principal difference is that for $NaNO_3$, there is no evidence for a continuum of inelastic scattering localized about the F point. Instead we find a component of inelastic scattering that is broad in both energy and wavevector, and with only a weak dependence on temperature.

Acknowledgments

The financial support of the EPSRC is gratefully acknowledged. One of us (MTD) is grateful to the staff of the Chalk River Laboratories for their kind hospitality and support for the triple-axis spectrometer measurements.

References

[1] Shinnaka Y 1964 *J. Phys. Soc. Japan* **19** 1281
[2] Schmahl W W and Salje E 1989 *Phys. Chem. Minerals* **16** 790
[3] Harris M J 1993 *J. Phys.: Condens. Matter* **5** 5773
[4] Lefebvre J, Fouret R and Zeyen C M E 1984 *J. Physique* **45** 1317
[5] Brooker M H 1978 *J. Phys. Chem. Solids* **39** 657
[6] Chisler E V 1969 *Sov. Phys.–Solid State* **11** 1032
[7] Karpov S V and Shultin A A 1976 *Sov. Phys.–Solid State* **18** 421
[8] Prasad Rao A D, Katujun R S and Porto S P S 1971 *Adv. Raman Spectrosc.* **1** 174
[9] Harris M J, Salje E and Güttler B K 1990 *J. Phys.: Condens. Matter* **2** 5517
[10] Lefebvre J, Currat R, Fouret R and More M 1980 *J. Phys. C: Solid State Phys.* **13** 4449
[11] Schmahl W W, Pintchovius L and Fuess H 1989 *Z. Kristallogr.* **186** 261
[12] Poon W C-K and Salje E 1988 *J. Phys. C: Solid State Phys.* **21** 715
[13] Reeder R J, Redfern S A T and Salje E 1988 *Phys. Chem. Minerals* **15** 605
[14] Lynden-Bell R M, Ferrario M, McDonald I R and Salje E 1989 *J. Phys.: Condens. Matter* **1** 6523
[15] Dove M T and Powell B M 1989 *Phys. Chem. Minerals* **16** 503
[16] Redfern S A T, Navrotsky A and Salje E 1989 *Contrib. Mineral. Petrol.* **101** 479
[17] Payne S J, Harris M J, Hagen M and Dove M T 1997 *J. Phys.: Condens. Matter* **9** 2423
[18] See, for example,
Bruce A D and Cowley R A 1981 *Structural Phase Transitions* (London: Taylor and Francis)
[19] Dove M T, Hagen M E, Harris M J, Powell B M, Steigenberger U and Winkler B 1992 *J. Phys.: Condens. Matter* **4** 2761
[20] Hagen M E, Dove M T, Harris M J, Steigenberger U and Powell B M 1992 *Physica* B **180+181** 276
[21] Steigenberger U, Hagen M, Caciuffo R, Petrillo C, Cilloco F and Sachetti F 1991 *Nucl. Instrum. Methods* B **53** 87
[22] Dorner B 1972 *Acta Crystallogr.* A **28** 319